Chapter 34

Three Dimensional Forms of Closely-Spaced Hydraulic Fractures

James Kear, Justine White, Andrew P. Bunger,
Rob Jeffrey and Mir-Akbar Hessami

Additional information is available at the end of the chapter

http://dx.doi.org/10.5772/56261

Abstract

When creating arrays of hydraulic fractures in close proximity, stress field changes induced by previously placed hydraulic fractures can lead to deflection in subsequent fracture paths and coalescence between fractures. Any fracture coalescence can compromise the effectiveness of the treatment array and the fracture geometry will not be appropriately accounted for in reservoir or caving models. Here we present the results of an experimental study consisting of arrays of 4 closely spaced hydraulic fractures grown sequentially in 350x350x350 mm blocks of a South Australian Gabbro under different initial stress states and for notched and un-notched wellbores. In particular we focus on insights gained from 3-dimesional serial sectioning and digital reconstruction of the hydraulic fracture patterns that were formed. The results show that the curving hydraulic fractures typically do not exhibit a high degree of radial symmetry in their paths even though the fractures grew by radiating outward from a centrally located wellbore. The results also confirm model predictions that a subsequent fracture will curve towards a previous fracture when the minimum stress is zero and that this curving is suppressed when the minimum stress is sufficiently large. Finally, fracture initiation is shown to be critical to the symmetry of the fracture pattern and preponderance of branching and therefore effective notches that lead to initiation in the eventual plane of favored propagation have a profound impact on the hydraulic fracture geometry.

Keywords: Hydraulic Fracturing, Closely Spaced Fractures, Serial Sectioning, Experiments

1. Introduction

The desired outcome of certain types of hydraulic fracture treatments is the creation of a system of closely spaced fractures. Forming such a closely spaced hydraulic fracture array is a highly effective technique for increasing the permeability of a rock mass [1,2] or reducing the strength of a rock mass in mining [3]. Application areas that benefit from an increase of permeability are those that value greater fluid conductivity such as tight gas extraction, in situ leaching, carbon sequestration and storage, geothermal power generation and similar activities. A reduction in the tensile and shear strength of the rock mass through the growth of hydraulic fractures is beneficial to block cave mining where earlier and more controlled caving events are preferable to uneven or irregular caving events caused by strong rock-masses not collapsing in a regular way under their own weight. In each application area, an optimal hydraulic fracturing treatment would provide the greatest alteration to the rock mass for the lowest cost.

When creating arrays of hydraulic fractures in close proximity, stress field changes induced by initial fractures can lead to deflection in subsequent fracture paths. Path deflection can compromise the effectiveness of the treatment array because it can lead to coalescence of the fractures rather than creation of distinct fractures. Also complex fracture paths such as coalescing or curving fractures may not be appropriately accounted for in reservoir or caving models. Ineffective treatments can be costly in terms of re-initiation and re-treatment remediation works. An accurate understanding of the interaction effects between multiple hydraulic fractures growing in close proximity to one another is therefore important for effective treatment design.

The 3-dimenional form of these fracture treatments can be difficult to observe in the field, and even in laboratory experiments often only a 2-dimensional cross-section of the fracture system is examined. In reality, the 3-dimensional nature of the fracture geometry is fundamental to the treatment performance in almost all industrial applications of hydraulic fracturing.

A recent numerical study [4] has identified a set of parameters controlling hydraulic fracture path deflection. The work presented here compares the results of an experimental study to the predictions of numerical modeling work with respect to the interaction effects of closely spaced hydraulic fractures. In this regard, the present work extends initial comparisons [5] to include a fully 3-dimensional characterization of the laboratory hydraulic fracture geometry.

The experimental study consists of closely spaced hydraulic fracture arrays grown in 350mm cubical sample blocks of a South Australian Gabbro. Four closely-spaced fractures were sequentially grown in each block under a variety of far-field stress and fluid injection conditions. After the experiments were completed the blocks were cut into 15 mm thick slices (serial sectioned) and the fracture paths were measured on the faces of these slices.

2. Experimental method

The 350x350x350 mm blocks were fabricated from Adelaide Black Granite (ABG), a gabbro from Black Hill Quarry in South Australia. This material has been used in previous hydraulic

http://dx.doi.org/10.5772/56261

fracturing experiments by CSIRO and the material properties of this rock have been well characterized and are listed in Table 1.

Fracture toughness	K_{IC}	2.3 MPa.m$^{0.5}$
Young's modulus	E	102 GPa
Poisson's Ratio	v	0.27
Tensile Strength	TS	9.4 MPa
Friction coefficient	f	0.45 (coarse finish) to 0.17 (polished finish)
Crystal Size		1-10mm diameter (typical)

Table 1. Adelaide Black Granite material properties.

Four hydraulic fractures were grown in each block, as shown in Figure 1. The fractures were grown one at a time beginning with the deepest fracture and working incrementally towards the top of the borehole.

The experimental setup used CSIRO's polyaxial load frame to apply confining stresses on the blocks along the vertical and horizontal axes. These stresses were applied using stainless steel flat jacks, inflated with water and with pressure controlled by three independent ISCO 260D syringe pumps.

Hydraulic fractures were grown by injecting fluid into an isolated section of the borehole in order to pressurize and initiate fracture growth. The Newtonian fluid consisted of a combination of water (13.6%), glycerol (80.0%) and blue food dye (6.4%) and had a dynamic viscosity of 0.058 Pa·s and a density of 1.21 kg/m^3.

The injection pressure was recorded upstream and downstream of a flow control (needle) valve that limits flow rate surges associated with injection system compressibility during breakdown and initial fracture growth. The temperature in the laboratory was stable at 20°C (± 1°C) and the temperature of the fracturing fluid was recorded through the tests to enable corrections for the effect of temperature on fluid viscosity.

Fracture initiation at a specific point in the borehole was achieved using an injection tool similar in concept to isolation packers used in the field (Figure 1, inset). O-ring "packers" isolated the fracture initiation zone above and below ports in the tool through which the fracture fluid exited the tool. In some blocks, a circumferential notch was scribed in the borehole at the location of fracture initiation, while in other tests the fractures were grown from an un-notched borehole.

After testing, the blocks were sectioned into 15 mm thick slabs, photographically scanned, and the fracture paths digitally re-constructed. The width of these slabs determined the resolution in one direction of the final re-construction.

After being cut, the slices were finished using a surface grinder to provide a smooth and clean face to allow the best possible observation of the hydraulic fracture paths.

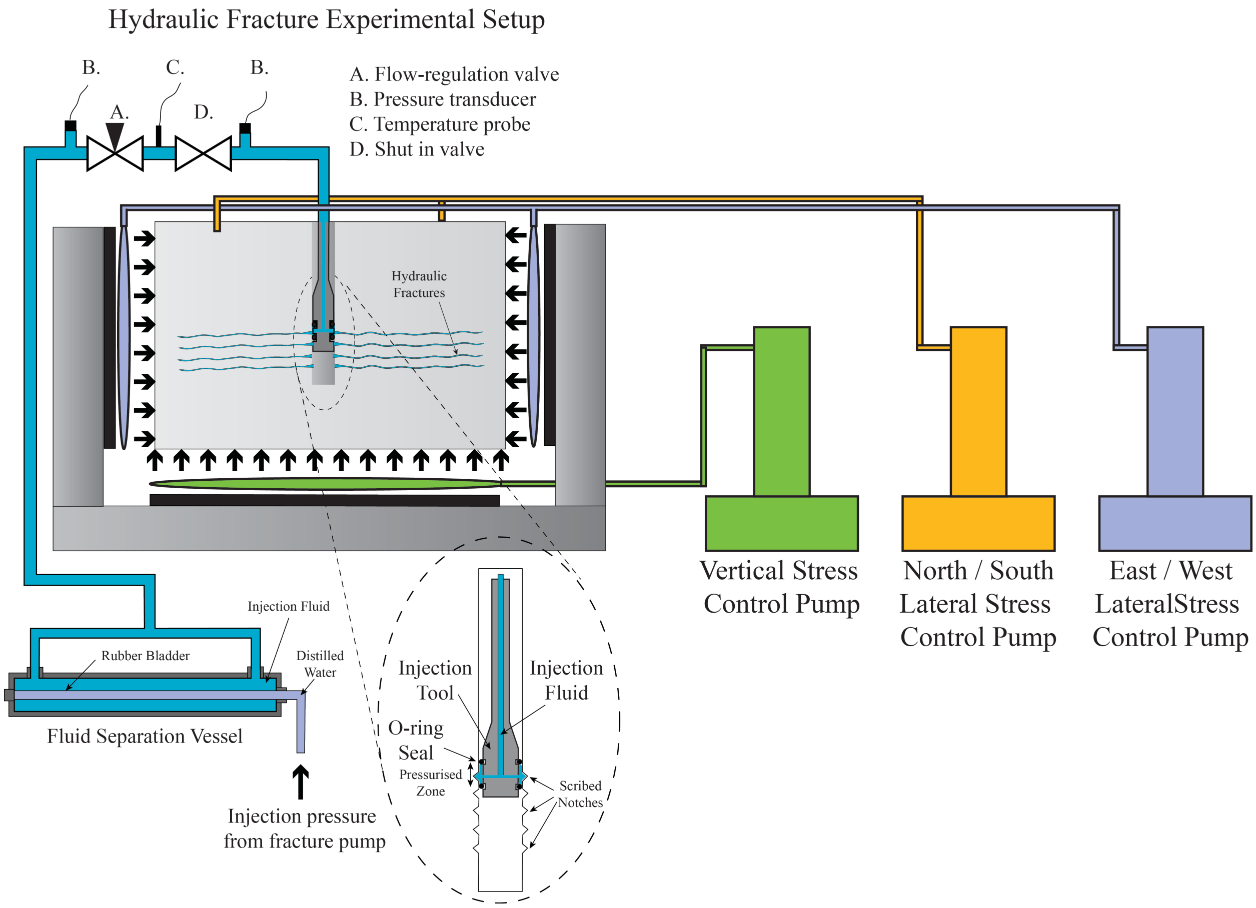

Figure 1. Hydraulic fracture experimental setup.

Each ground face was treated with a penetrant crack detection dye to highlight the fracture path. (This penetrant dye is sold commercially for detection of cracks in metal structures such as brake rotors.) Slices were digitally photographed at a high resolution under controlled lighting conditions to allow precise determination of fracture locations

Final images of the slice faces have a resolution of approximately 8 pixels/mm. The digitized trace of the hydraulic fracture paths are then re-constructed in three dimensions, after accounting for the material removed by the saw blade thickness and by grinding, by laying out these traces as per their original spatial locations in the block. In this way a 3-dimensional image of the fracture system is obtained.

3. Results

The results from three hydraulic fracturing experiments are presented for comparison. An analysis of 2-dimensional cross sections for these three cases was presented in Ref [5]. All three experiments are cases where four sequential hydraulic fractures have been grown in close proximity, all are in the same size block (350mm on each side) and all fractures for all 3 blocks were grown using the same fluid and injection rate.

http://dx.doi.org/10.5772/56261

The test parameters of the first 2 experimental cases (Block 3 and Block 4) were designed such that the minimum (in this setup, the vertically directed) stress was small enough so that the tensile stresses produced near the tip of each propagating hydraulic fracture would be expected to generate a small region of re-opening on the neighboring, previously-placed hydraulic fracture. The model predictions [5] show that in this case the growing hydraulic fracture is predicted to curve towards the previously placed hydraulic fracture, that is, it exhibits “attractive curving”. Hence, this is the predicted behavior for both Blocks 3 and 4, which are identical with the exception of the existence of fracture initiation notches scribed in the borehole of Block 4. Furthermore, it was expected from previous experiments for curving hydraulic fractures (grown near a free surface)[6], that the fractures would form roughly axisymmetric bowl-shapes.

In the third case (Block 6), the experimental parameters were chosen in such a way as to suppress the re-opening of the previous hydraulic fractures through the application of a significant minimum (vertical) stress (acting against the opening of the fractures). In this case, numerical modeling [5] predicts that the fractures would grow parallel to one another up to a length commensurate with the specimen size. Details of experimental parameters are presented in Table 2 below, recalling that rock material properties are given in Table 1.

		Block 3	**Block 4**	**Block 6**
Maximum principal stress	σ_{max}	4.6 MPa	4.6 MPa	18 MPa
Minimum principal stress	σ_{min}	0 MPa	0 MPa	14.4 MPa
Borehole radius	R	8 mm	8 mm	8 mm
Initial fracture spacing along borehole	H	15 mm	15 mm	25 mm
Fracture fluid dynamic viscosity	μ	0.58 Pa.s	0.58 Pa.s	0.58 Pa.s
Borehole notch depth		(no notch)	~3 mm	~3 mm
Volumetric injection rate	$\bar{Q}$	0.19 ml/min	0.19 ml/min	0.19 ml/min
Residual fracture widths*	w_o	~1 μm	~1 μm	~1 μm
Fracture half length	α	175 mm	175 mm	175 mm
Reopening of previous fracture [5]		Predicted	Predicted	Suppressed

Table 2. Experiment parameters for presented cases.

Note that the residual widths of the fractures in these experiments are difficult to quantify accurately. No proppant was included in the fracture fluid and the fluid viscosity was low. The residual widths have been selected in the model calculation so that there would be little effect exerted on the stresses in the surrounding rock, although the results subsequently presented do suggest some impact on the stresses did occur in some of the experiments, as evidenced by an increase in breakdown pressure for each sequential fracture.

3.1. Case 1 (Block 3) un-notched zero vertical stress

In Block 3 the hydraulic fractures were grown from an un-notched borehole under conditions where the previous fractures were predicted to re-open because of the tensile stresses surrounding the tip of the propagating fracture.

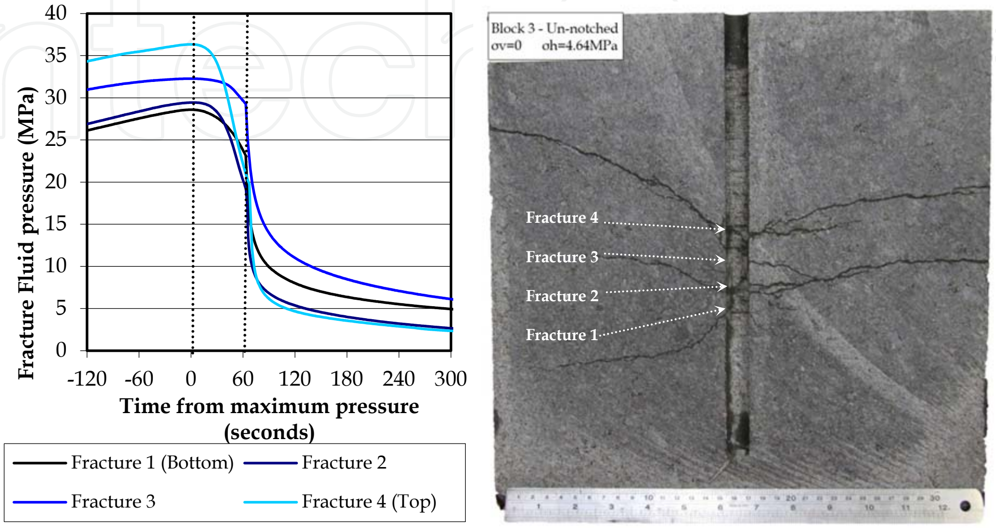

Figure 2. Fracture pressure records (the vertical dotted lines represent maximum pressure and shut in respectively) and 2-dimensional cross section of Block 3 (Hydraulic Fractures can be seen as dark grey cracks on the cross-section image), after Bunger et al. [5].

The pressure records for each of the four hydraulic fractures in the block are presented on the left in Figure 2 with zero time shifted to correspond to the maximum pressure reached during each injection. For each fracture, pumping was maintained at a constant rate throughout pressurization, breakdown and for 60 seconds after the maximum pressure was reached. After 60 seconds the pump was stopped and the fracture was shut in (valve closed) to allow fluid pressure in the fracture to fall off naturally for a few minutes before venting the system to atmospheric pressure. The next fracture was then commenced approximately one hour after the previous fracture was shut-in. For all fractures the breakdown (maximum) pressure of each subsequent fracture is greater than that of the fracture that preceded it. This is possibly an indication of some residual change in the local stress locked in from the previous fracture growth that falls off over the hours following the experiment as the viscous fluid slowly flows back to the wellbore. This effect is significantly more pronounced for this un-notched case (Block 3) than for the case where the borehole was notched at the fracture initiation locations (Block 4, next section).

As can be seen on the right in Figure 3, the fracture paths are not symmetric about the borehole and the fracture pattern appears to be characterized by many small branches, deviated paths, and coalescence of the fractures from the 4 initiation points to form two dominant fractures going to the right and three dominant fractures going to the left. 3-dimensional reconstruction shows that this reduced number of fractures due to coalescence occurred throughout the block.

http://dx.doi.org/10.5772/56261

The lack of radial symmetry in the curving fracture paths in this case is not surprising. There were no notches to provide for fracture initiation in the plane of preferred propagation. Rather, a close inspection of the near borehole region in Figure 3 shows that the hydraulic fractures initiated at a small angle to the wellbore axis. The fractures then re-oriented as they grew so as to be favorably oriented relative to the applied stresses. But given that initiation was not axisymmetric, the fact that growth was non-axisymmetric is to be expected. Instead, these fractures exhibit approximate translational symmetry along the direction of viewing in Figure 3 (perpendicular to the page), where we note that this direction is parallel to the plane of the high angled initiation. Also, the apparent "repulsive" nature of the curving, which is in contrast to predictions for the stress based modeling of initially parallel fractures (as in Block 4, next section), probably arises directly from the high angled initiation geometry. Finally, re-orientation of a 3-dimensional hydraulic fracture is certain to produce complex, mixed-mode loading of the crack tip, which is well-known to result in segmentation of fracture planes [7,8]. Hence it seems that most of the features of the observed fracture patterns in this block can be related to the initiation geometry.

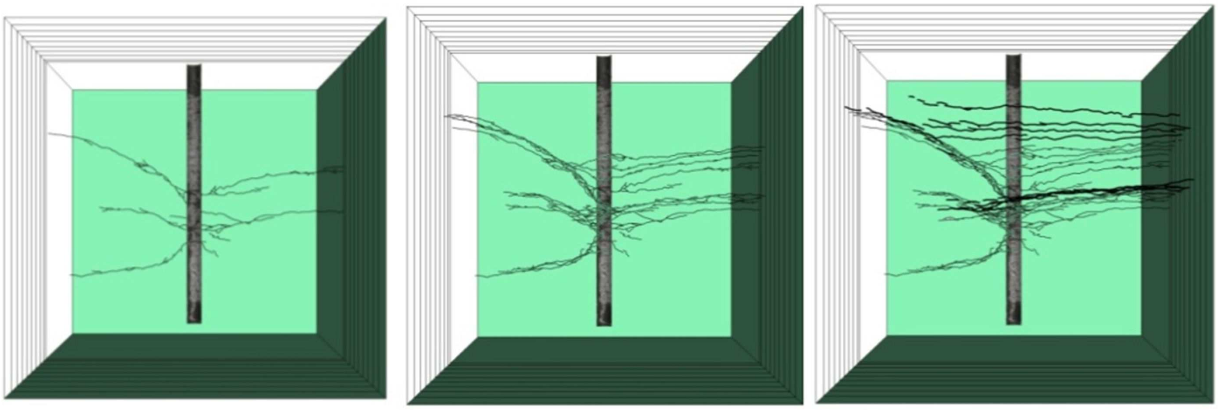

Figure 3. dimensional reconstruction of Block 3 with increasing number of slices represented, single central slice (Left), 50mm of block reconstructed (middle), 150mm of block reconstructed (right).

3.2. Case 2 (Block 4) notched no vertical stress

Block 4 was tested under identical conditions to the first case (Block 3), however for Block 4, circular notches approximately 3 mm deep were scribed into the borehole at the hydraulic fracture initiation locations. Hydraulic fractures grown from a borehole which does not contain notches tend to breakdown in a vertical orientation, consistent with the stress concentration around a circular wellbore, and then re-orient to the principal stress direction. Borehole notches provide a stress concentration location that aids in the initiation of a horizontal fracture aligned with the principal stress direction. Fractures initiated from notches are expected to have fewer branches and to be more predictable in their behavior, which is demonstrated by the results presented here.

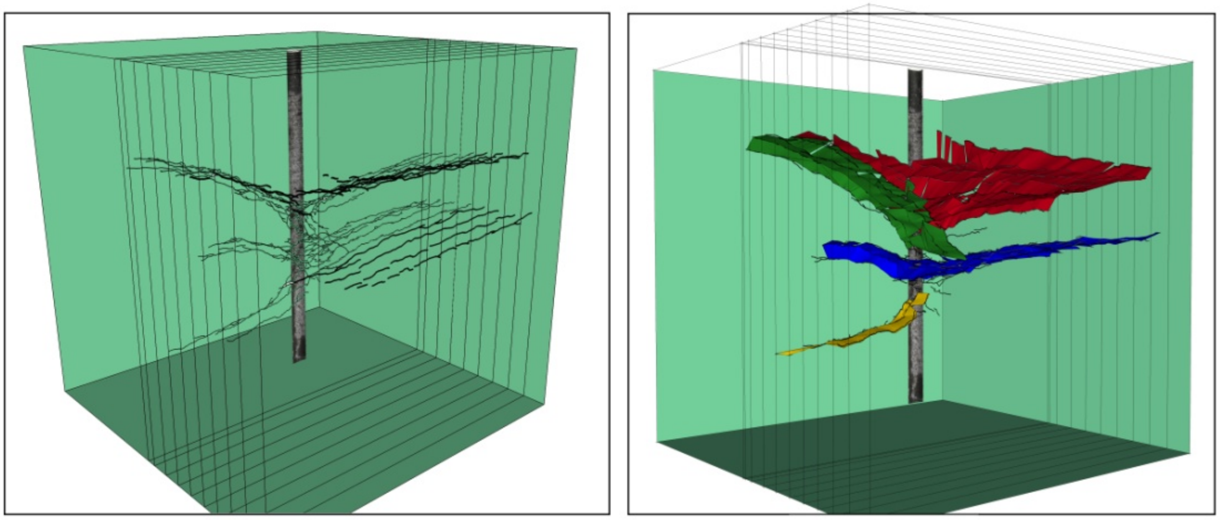

Figure 4. Different viewing angles of the fracture paths in Block 3. Raw traces are presented on the left and fitted mesh surfaces representing fractures on the right (a video animation of this fracture can be viewed at http://youtu.be/7ykr_Jg-VcU).

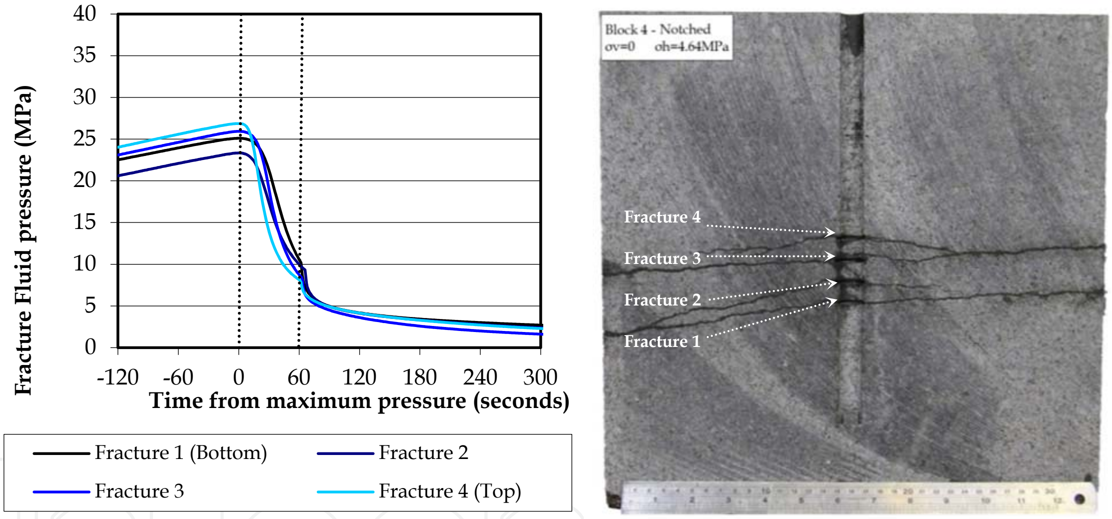

Figure 5. Fracture pressure records and 2-dimensional cross section of Block 4, after Bunger et al. [5].

Pressure records for Block 4 are presented on the left in Figure 5. It is interesting to note that the breakdown (maximum) pressures were lower in every fracture than those observed in Block 3 (un-notched borehole case). Again the maximum pressures are generally observed to become incrementally higher, however this effect is less pronounced than in the un-notched Block 3.

For these stress and injection conditions, numerical modeling [5] predicts that the fractures will coalesce and eventually join at between 5 and 10 times the initial fracture spacing. Examination of Figure 5 shows that the observed behavior is consistent with the prediction, with fracture 2 coalescing with the previously placed fracture 1 at a radial distance equal to about 10 times the initial spacing and fracture 4 coalescing with the previously placed fracture 3 at a radial distance equal to about five times the initial spacing.

If indeed these curving hydraulic fractures grew in an axisymmetric manner, then the final shape of fractures 2 and 4 would be like an inverted bowl. However, the curving was instead more fold-like and thus formed inverted troughs. Hence, one of the surprising results of these experiments (that is evident only via the 3-dimensional reconstruction) is that hydraulic fractures that essentially radiate from the wellbore and would likely have been radially symmetric in plan view, at least for a substantial portion of their propagation, do not necessarily maintain radial symmetry in their curving behavior. For fracture 4 in particular, the curving exhibits approximate translational symmetry along the direction of viewing in Figure 6. That is, fracture 4 curves toward fracture 3 in the projected plane shown in Figure 6 significantly more strongly than it curves toward fracture 3 in the direction perpendicular to the page. Fracture 2, on the other hand, appears to curve towards fracture 1 in both planes (closer to radial symmetry than fractures 3 and 4), however the curving is much stronger in the plane of the page than it is in the direction perpendicular to that plane. Further experimentation is aimed at determining the conditions that lead to this scenario and ascertaining whether axisymmetric curving can be attained under these experimental conditions as it is under near-surface conditions in the experiments of [6].

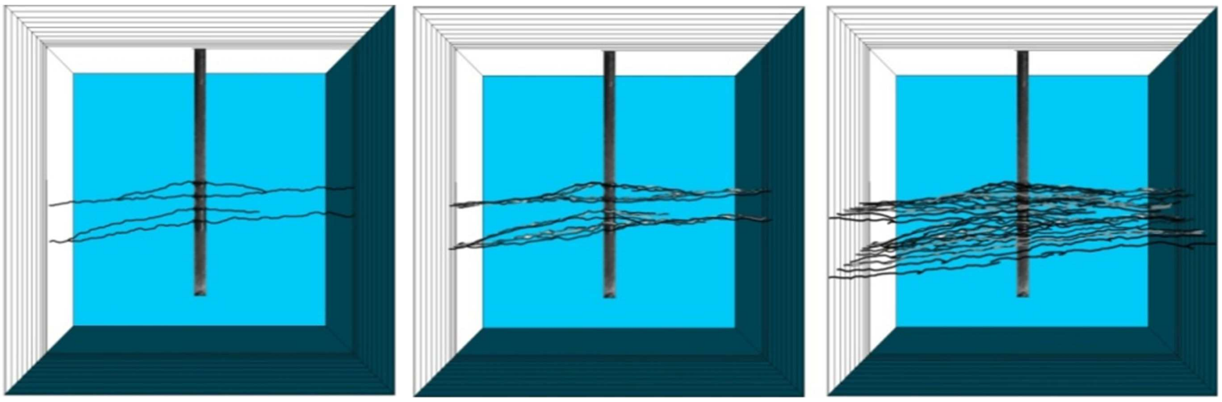

Figure 6. dimensional reconstruction of Block 4 with increasing number of slices represented, single central slice (Left), 50mm of block reconstructed (middle), 150mm of block reconstructed (right).

The observed approximate translational symmetry is one of the few similarities between the notched Block 4 and the un-notched Block 3. In contrast, the curving is attractive in Block 4 and there are few branches in the fracture path.

The translational symmetry can again be seen in Figure 7 where fracture 4 (yellow) can be seen strongly curving towards fracture 3 (pink) in the plane of original sample sectioning to the left of the borehole. In contrast, fracture 4 (yellow) essentially grows parallel to fracture 3 (pink) in the re-constructed plane perpendicular to the original cut which can be seen to the right of the borehole in Figure 7. This effect is repeated however more subtly for fractures 1 (orange) and 2 (green).

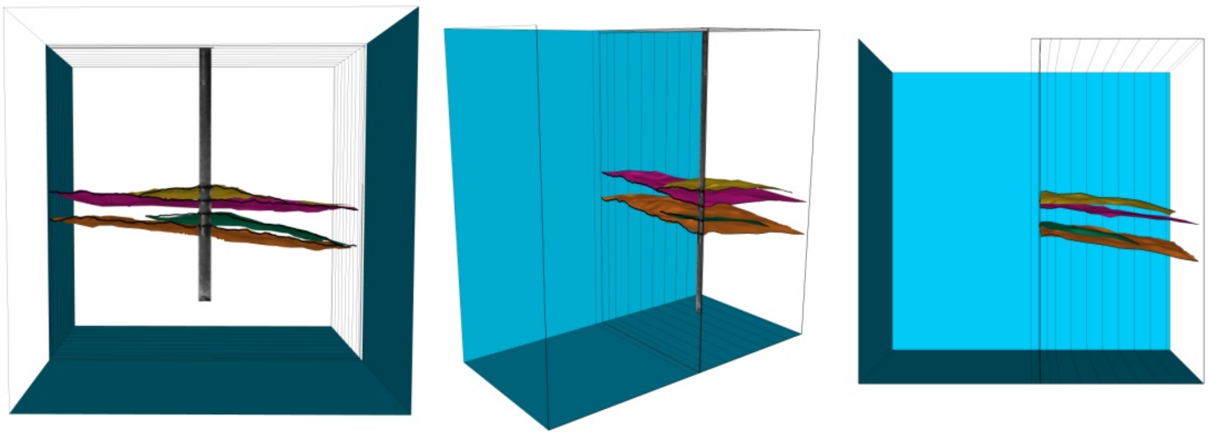

Figure 7. Rendered fracture paths in Block 4. Original fracture trace shown in the left image and re-constructed cross-section (oriented at 90 degrees to the original) in the right image. A composite of the original and re-constructed cross-sections is presented in the central image. A video animation of this fracture can be viewed at http://youtu.be/KMioXgoKfrg).

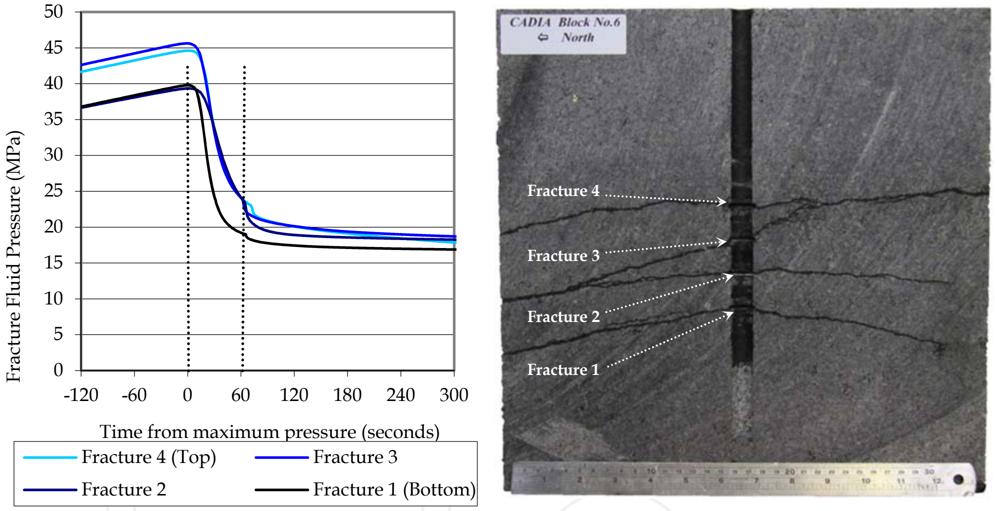

Figure 8. Fracture pressure and 2-dimensional cross section of Block 6, after Bunger et al. [4].

In Figure 7, fractures 1 (orange) and 3 (pink) can be observed appear to be clipped along a plane. This is due to the fact that these two fractures extend to the edges of the sample. This effect can be clearly seen in the uploaded animation linked in the Figure 7 caption.

3.3. Case 3 (Block 6) notched with substantial vertical stress

In Block 6 there was sufficient applied vertical stress, as predicted by the model, to suppress re-opening of existing fractures thus enabling the closely spaced fractures to grow parallel to one another without coalescence.

As can be seen in Figure 8, fractures 1, 2 and 4 appear to grow roughly parallel to one another and perpendicular to the minimum principal stress (which is vertical). Fracture 3, however,

http://dx.doi.org/10.5772/56261

does not initiate cleanly at the notch and thus grows at an angle of approx 35 degrees away from the principal stress direction. Possible reasons for this may be poor notch quality, localized material property changes or initiation at an existing micro crack (see a more detailed discussion in ref [4]).

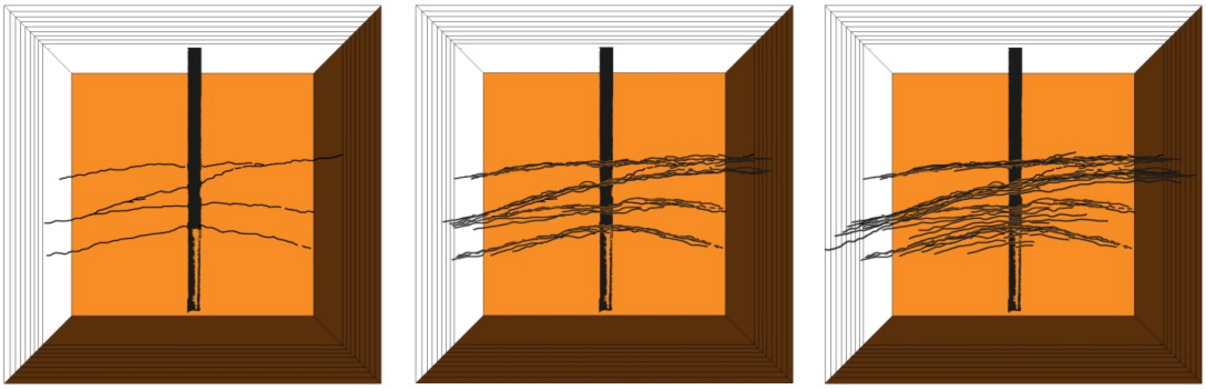

Figure 9. dimensional Reconstruction of Block 6 with increasing number of slices represented, single central slice (left), 50 mm of block reconstructed (middle), 150 mm of block reconstructed (right).

It is interesting to note that the breakdown pressures for the first two fractures are nearly identical, while fracture 3 had a higher breakdown pressure that is consistent with it not initiating at the notch as mentioned above. Fracture 4 also had a higher breakdown pressure, which is possibly due to fracture three growing close to the point of initiation of fracture 4 so that the residual width of fracture 3 affected the stress field in the initiation region of fracture 4.

The 3-dimensional re-construction of Block 6, Figures 9 and 10, confirms that fractures 1, 2 and 4 grow roughly planar and parallel to one another. We can also see that fractures 1, 2 and 4 maintain a roughly horizontal orientation, dipping slightly as they come forward out of the page. Fracture 3, which did not break down at the notch cleanly and thus began on a greater angle than the other fractures, appears to re-orient itself on the left side of the borehole. However, on the right fracture 3 appears to grow into the zone of influence of fracture 2 and be drawn towards it, eventually coalescing at approximately 4 times the fracture spacing.

The anomaly of fracture 3 aside, in this case the fractures are observed to propagate parallel to one another, and with the fewest branches in the fracture paths of the 3 blocks we tested. In fact as can be seen in the 3-dimensional reconstruction in Figure 10, when viewing the re-constructed cross section (to the right of the borehole) all four fractures are seen to grow parallel to one another. The parallel propagation is consistent with the model predictions for these stress and injection conditions [4,5]. The reduction in branches is beyond the scope of the modelling, but is to be expected when the fractures are not curving since the curving is associated with mixed mode loading at the crack tips that can also be associated with crack tip segmentation [7,8].

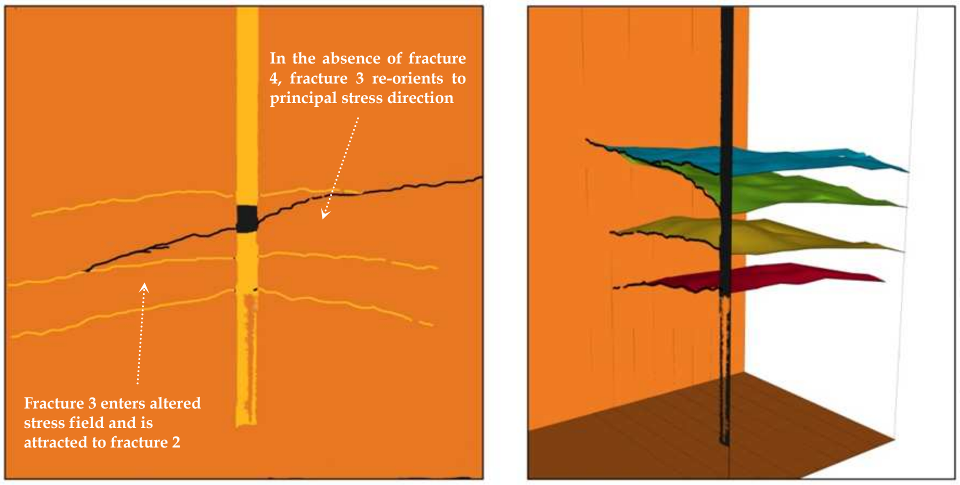

Figure 10. A 2-dimensional cross-section of Block 6 showing the deflected path of fracture three (left) and a 3-dimensional reconstruction of the fracture paths in Block 6 (a video animation of this fracture can be viewed at http://youtu.be/ZCMBWGl_8-Y).

4. Experimental practicalities and future work

A significant amount of time is currently required to produce the final 3-dimensional digital images of the fractures using serial sectioning. The most time consuming steps in the process are cutting the blocks into sections and scanning and processing the fracture images. Several attempts at developing and applying existing algorithms to extract the fracture geometry from a digital image were made, but without success. In particular, for our application and in our experience, we found that line-tracing type algorithms that have been used in applications such as X-ray Computer Tomography trade off precision in the tracing for the sake of high throughput. This makes sense when one has many, very closely spaced and easily acquired cross-sectional images to analyze. However, in our case a significant time investment is required to obtain each cross-sectional image and so our priority is on accuracy rather than throughput. Hence, a manual method was finally settled on because it gave the most accurate and detailed digital fracture image from each rock slice. But, if this part of the process could be automated, significant savings in overall time needed would be achieved.

Having a 3-dimensional representation of a hydraulic fracture is very useful, but to obtain full benefit this image should be viewed using an interactive 3-dimensional computer application. Presenting static views of the fracture, as was done in this paper, limits the benefit. Improvements to the 3-dimensional images, such as advanced highlighting and shading methods, will be investigated as a way to improve the static images for publication.

In the future, in addition to running several replications of the tests described here, we see significant potential in applying serial sectioning as part of studies of fracture initiation at notches in the borehole to better understand the effect of initiation geometry on near-, intermediate- and far-field fracture geometry. A series of tests in a finer-grained rock material is seen as part of this proposed work. Understanding how to better initiate fractures so that an array of parallel hydraulic fractures can be grown transverse to the borehole is important in mining, petroleum, and geothermal application areas.

5. Conclusion

Reconstruction of fracture paths from tested blocks gives additional insight into fracture growth and is a useful technique for extracting additional information from tested blocks. In the study presented here, the 3-dimensional reconstructed fracture images have been used to show that the curving fracture geometries resulting from sequential growth of closely spaced, interacting hydraulic fractures exhibit translational symmetry even though the hydraulic fracture growth radiated from a centrally located wellbore. While based only on a few experiments and therefore in need of further experimental confirmation, this unexpected result is important for selection of appropriate simplifying symmetry assumptions (i.e. plane strain versus radial symmetry) in numerical models.

In addition to this conclusion, which is fundamentally based on 3-dimensional considerations, these reconstructions have confirmed the consistency between model and experiment that Bunger et al. [4] draw based on a single cross section of these fractures, namely that a subsequent fracture will curve towards a previous fracture when the minimum stress is zero and that this curving is suppressed when the minimum stress is sufficiently large. Also, the 3-dimensional reconstructions confirm that fracture initiation is critical to the symmetry and preponderance of branching. Therefore, cutting effective notches in the borehole that facilitate fracture initiation in the eventual plane of favored propagation have a profound impact on the hydraulic fracture geometry.

Serial sectioning and digital 3-dimensional image reconstruction is found to be an effective method to obtain a more complete understanding of fracture geometry and interaction. Once the fracture traces are assembled into a 3-dimensional model, the fracture image can be rotated in space and viewed from different directions, which allows detailed examination of the fracture geometry and spatial relationship between fractures. It is, however, time consuming and therefore relatively expensive, but no other method provides the level of detail or the ability to image fractures in large rock blocks.

Acknowledgements

The authors thank both CSIRO and Newcrest Mining Limited for funding the experiments and for permission to publish. Serial sectioning comprised a portion of the final year thesis for JW at Monash University under the supervision of MAH. Online animations were prepared by JK and Dane Kasperczyk (CSIRO Earth Sciences and Resource Engineering, Clayton, Australia).

Author details

James Kear[1*], Justine White[1], Andrew P. Bunger[1,2], Rob Jeffrey[1] and Mir-Akbar Hessami[3]

*Address all correspondence to: James.Kear@csiro.au

1 CSIRO Earth Sciences and Resource Engineering, Clayton, Australia

2 Department of Civil & Environmental Engineering, University of Pittsburgh, Pittsburgh, Pennsylvania, USA

3 Department of Mechanical and Aerospace Engineering, Monash University, Clayton, Australia

References

[1] King, G. E. Thirty years of gas shale fracturing: What have we learned? In Proceedings SPE Annual Technical Conference and Exhibition. Florence, Italy. SPE 133256, 2010.

[2] Rodrigues, V. F., L. F. Neumann, D. Torres, C. Guimaraes, and R. S. Torres, 2007. Horizontal well completion and stimulation techniques - A review with emphasis on low-permeability carbonates. In Proceedings SPE Latin American and Caribbean Petroleum Engineering Conference. Buenos Aires, Argentina. SPE 108075.

[3] van As, A. and R. Jeffrey. Caving induced by hydraulic fracturing at Northparkes Mines. In Pacific Rocks 2000 - Proc. 4th North American Rock Mechanics Symposium, eds. J. Girard, M. Liebman, C. Breeds, and T. Doe. Seatle, WA: Balkema, 353–360, 2000.

[4] A. P. Bunger, X. Zhang, and R. G. Jeffrey, "Parameters Affecting the Interaction Among Closely Spaced Hydraulic Fractures," *SPE Journal*, no. March, 2012.

[5] A. P. Bunger, R. G. Jeffrey, J. Kear, X. Zhang, and M. Morgan, "Experimental Investigation of the Interaction Among Closely Spaced Hydraulic Fractures," in *American Rock Mechanics Symposium*, 2011.

[6] Andrew P. Bunger, Robert G. Jeffrey and Emmanuel Detournay, "Evolution and morphology of saucer-shaped sills in analogue experiments (in Structure and emplacement of high-level magmatic systems)" Geological Society Special Publications (2008), 302:109-120

[7] Hodgdon, JA & Sethna, JP, 'Derivation of a general three-dimensional crack-propagation law: A generalization of the principle of local symmetry' Physical Review B Condensed Matter, vol 47, no. 9, pp. 4831-4840, 1993.

[8] Leonid N. Germanovich, Dmitriy K. Astakhov, Michael J. Mayerhofer, Jacob Shlyapobersky, Lev M. Ring, Hydraulic fracture with multiple segments I. Observations and model formulation, International Journal of Rock Mechanics and Mining Sciences, Volume 34, Issues 3–4, April–June 1997, Pages 97.e1-97.e19

IntechOpen